ANALYSIS OF NO-FLOW BOUNDARIES IN MIXED UNCONFINED-CONFINED AQUIFER SYSTEMS

A Thesis

by

KENT LANGERLAN

Submitted to the Office of Graduate Studies of
Texas A&M University
in partial fulfillment of the requirements for the degree of

MASTER OF SCIENCE

December 2009

Major Subject: Geology

ANALYSIS OF NO-FLOW BOUNDARIES IN MIXED UNCONFINED-CONFINED AQUIFER SYSTEMS

A Thesis

by

KENT LANGERLAN

Submitted to the Office of Graduate Studies of
Texas A&M University
in partial fulfillment of the requirements for the degree of

MASTER OF SCIENCE

Approved by:

Chair of Committee,	Hongbin Zhan
Committee Members,	Chris Mathewson
	John R. Giardino
Head of Department,	Andreas Kronenberg

December 2009

Major Subject: Geology

ABSTRACT

Analysis of No-Flow Boundaries in Mixed

Unconfined-Confined Aquifer Systems. (December 2009)

Kent Langerlan, B.A., SUNY Geneseo

Chair of Advisory Committee: Dr. Hongbin Zhan

As human population increases, demand for water supplies will cause an increase in pumping rates from confined aquifers which may become unconfined after long-term pumping. Such an unconfined-confined conversion problem has not been fully investigated before and is the focus of this thesis. The objective of this thesis is to use both analytical and numerical modeling to investigate groundwater flow in an unconfined-confined aquifer including the no-flow lateral boundary effect and the regional flow influence. This study has used Girinskii's Potential in combination with MATLAB to depict how changes in aquifer dimensions, hydraulic properties, regional flow rates, and pumping rates affect the size and shape of the unconfined-confined boundary. This study finds that the unconfined-confined conversion is quite sensitive to the distance between the piezometric surface and the upper confining bed when that distance is small, and the sensitivity lessens as that distance increases. The study shows that pumping rate is the dominating factor for controlling the size of the unconfined-confined boundary in comparison to the regional flow. It also shows that the presence of a no-flow boundary alters the normally elliptical shape of the unconfined-confined boundary.

DEDICATION

To my parents, Bruce and Linda Langerlan, and sister, Lisa Andrews

ACKNOWLEDGEMENTS

I would like to first thank Dr. Hongbin Zhan for guiding and supporting me during my research. His teachings and intelligence assisted in my personal growth and academic development during the last three years while under his advisement. Because of his faith in me, I am able to present this research.

To my parents Bruce and Linda Langerlan: my unending thanks and love for all you have done for me. Your constant love and faith in me could be felt across the country. Completing my research could only be possible because of your support.

To my sister, Lisa Andrews: thanks for being just a phone call away. There is no other person that I can count on more than you. Your constant advice and occasional reminders have kept me down to Earth and dedicated to my studies, as well as helped me mature into the person I am today.

To my friends Shawn Murphy, Navina Bhatkar and Sean Coles: thanks for showing me what true friends are. When I have needed a place to go or a person to depend on you have always answered the call. I will always be there for you.

Lastly, I would like to thank the faculty, staff, and committee members that aided me during my graduate studies. I have learned much from your wisdom and guidance. Know that I will always view my experiences here with gratitude and appreciation.

TABLE OF CONTENTS

Page

LIST OF FIGURES

CHAPTER I

INTRODUCTION AND GENERAL OVERVIEW

The study of hydrogeology has become increasingly important as groundwater reserves are continuously consumed by an increasing human population for potable water and irrigation. The understanding of complex groundwater flows has become vital to sustaining humanity and the environment it inhabits. Whereas significant strides have been made to better understand how groundwater travels through the subsurface, assumptions are made to make quantitative results easier to calculate which induces error.

A large amount of research within hydrogeology focuses upon the quantitative description of flow within a single confined or unconfined aquifer to determine discharge, hydraulic conductivity, and hydraulic head. The ability to estimate and apply these variables increases the understanding of the complexities of groundwater flow. The result is an improved accuracy in modeling groundwater flow that is useful in water management. The understanding of groundwater flow dynamics has become even more necessary as emphasis within the last few decades has been placed upon high yield wells

---

This thesis follows the style of *Ground Water*.

instead of a more optimal use of several wells across the span of an entire aquifer (Birtles and Reeves, 1977).

Whereas equations such as Darcy's Law and Theis' Equation prove useful for a basic understanding of the relationship between variables such as flow and hydraulic conductivity, they are used in aquifers where many assumptions must be made. The assumptions made usually refer to a confined or unconfined aquifer to be homogeneous, infinite and perfectly horizontal systems. One assumption that is commonly made restricts any theoretical or actual aquifer to be restricted to either a confined or unconfined scenario with no possibility that a transition occurs (Elango and Swaminathan, 1980).

Girinskii's Potential has been proposed as a quantitative method to predict unconfined-confined boundaries within a steady-state aquifer and has been successfully applied by Chen et al. (2006) but is limited to a mixed unconfined-confined aquifer near a constant head boundary. The purpose of this investigation is to include other environmental factors such as regional flow and no-flow boundaries and to create a model using Girinskii's Potential which allows for rapid calculation and 2-D visualization of unconfined-confined boundaries. The improved model may allow for the estimation of sustainable pumping rates within a variety of confined aquifers which could prevent overpumping and exhaustion of groundwater resources.

1.1 Effects of Unsustainable Pumping

The unconfined-confined system within a normally confined aquifer has been largely overlooked as the qualitative and quantitative methods within hydrogeology generally rely on either a confined or unconfined aquifer.

One complex situation in which traditional equations may not prove adequate can be found within confined aquifers with pumping rates that greatly exceed recharge rates. Where typically a confined aquifer contains enough pressure to maintain the piezometric surface high above the upper confining bed, increased pumping rates may decrease the surface to such an extent that the cone of depression falls below that boundary. This would create a zone around the pumping well where the generally confined aquifer becomes unconfined. This transition from confined to unconfined creates a situation where traditional equations such as Dupuit's equation or Theis' equation fail to adequately describe groundwater flow around the well (Chen et al., 2006). Such a transition is enhanced when there are no-flow boundaries such as faults or bedrock near the pumping well.

Evidence of excessive pumping rates affecting confined aquifers has been reported in many places in the world including the Great Lakes region within which areas of Michigan, Illinois, Ohio, and Montana are the most affected. Walton (1964) studied a carbonate sandstone aquifer known as the Cambrian-Ordovician aquifer that has a thickness greater than 1,000 feet and is located in the Chicago, Illinois region. The purpose was to presented data and address concerns with regards to increases in pumping since the late 1800's, when the original well was artesian and flowed at 150

gallons/minute (Visocky, 1982). Walton (1964) showed the correlation between increased industrial and residential usage of water supplies and aquifer depletion. The data included information from six major areas in the Chicago region where water levels declined within the aquifer between 7 and 18 feet per year in non-pumped areas. It was estimated that in the Chicago area alone a 216 feet decline in the water level in non-pumped areas has occurred between 1864 through 1958 with a maximum of 650 feet decline in water level at the pumping site. Walton (1964) then predicted that if the rate of pumping from the aquifer continued at the rates he analyzed, that the aquifer would dewater and lose up to 26% of its productivity. Future pumping rates were predicted to increase from 96.5 million gallons/day in 1961 to 243 million gallons/day by 2010. Walton (1964) foresaw the need for alternative water sources and recommended utilizing vast reserves of freshwater from Lake Michigan.

Visocky (1982) continued Walton's work in studying the Cambrian-Ordovician aquifer by examining the impact Lake Michigan waters had on groundwater dependency. The concern was that excess pumping occurring at a rate of 180% the sustainable level would dewater the aquifer and reduce its production. Visocky (1982) noted that Chicago's use increased dramatically since Walton's work, and the total water level decrease had exceeded 900 feet. In addition, dewatering was evident in the uppermost areas of the Cambrian-Ordivician aquifer. The results from the model suggested that continued pumping from the Cambrian-Ordivician aquifer would result in reduction of the water levels within the aquifer, and the water level decline would be approximately 100 to 400 feet along the Wisconsin border by 2020. Areas such as Joliet

would eventually lose 19% of its total pumping capacity by 2020 if the trends continued, however, other areas such as Aurora would have a reduction of 34% by 1990. Areas such as northern Cook County, which is allocated Lake Michigan water, had high cones of depression yet the water level may recover up to 300 feet by 2020. Visocky (1982) suggests that areas with critical water levels should reduce pumping and use the waters from the Great Lakes, and predicted that by supplementing the water supply with Lake Michigan water the aquifer could be used without further harm.

Naymik (1979) evaluated the Maumee River drainage basin which is located primarily in northwestern Ohio, but also includes sections in Indiana and Michigan. The aquifer consists of glacial till from the Wisconsin glaciation which filled in river valleys and allows a high hydraulic conductivity and recharge to be possible. Naymik (1979) used information gathered from the Ohio Division of Water, potentiometric data and pumping rates based upon historic, accelerated, and peak usage to predict the effects of continued use of the Maumee aquifer between the years of 1986 and 2036, in intervals of ten years. The data gathered suggested that there would be minor changes in the piezometric surface by the year 1986, but continued use would eventually cause increased drawdown and the spreading of the unconfined-confined cones around pumping wells by 2006. The model also predicted 25 feet of head decline in Ohio, notably in areas such as St. Mary's and Findlay. By 2026 eight more areas would exhibit similar declines. Naymik (1979) mentioned that by 2036 the regional severity of the effects caused by increased rates of pumping would be lessened because of the highly permeable glacial till. Several areas with heavy levels of economic development

would be effected more severely and could expect extreme drawdowns and suffer shortages of water. Lima, Ohio was predicted to have a water decline of 200 feet by 2006 as a result of pumping rates estimated to be ten times greater than the recharge rate. Findlay, Ft. Wayne, and Toledo were predicted to suffer from decreased water levels and would not be able to sustain the estimated water usage by 2036. To prevent this outcome Naymik (1979) recommended careful examination of increased pumping rates and the effect that they cause to the Maumee aquifer, and further development of wells in areas with a high recharge. Continued groundwater resource appraisal would also lead to new groundwater reserves to ease the burden of increased development of the area which depends on the aquifer (Naymik, 1979).

1.2 Development and Use of Hydrogeological Models

Kashef (1971) was one of the first to examine how large pumping rates from over-pumped wells can create a unconfined-confined boundary using a force-potential concept and also considered vertical components of aquifer flow in his model.

Rushton and Turner (1975) realized that heavy pumping could create an unconfined-confined aquifer. He applied a numerical method to predict unconfined-confined areas within an aquifer. Rushton and Turner (1975) also included infiltration in his model. According to Rushton and Turner (1975), for greater pumping rates the finite difference method followed the general pattern of Theis' Curve, but he found that the solution was inaccurate when predicting the amount of dewatering and the time taken for

drawdown to occur. For example, Theis' Equation did not allow for various environment conditions such as infiltration and did not compensate for reduction of saturated depth. Birtles and Reeves (1977) improved the Theis' model to take into account the transition from confined to unconfined but the result was a model that was applicable on a regional scale.

Similar solutions such as in Moench and Prickett (1972) were developed for a confined aquifer transitioning into a water table aquifer. These equations were derived from analogous heat flow equations and are based upon similar theories as Theis' equation. After a pumping test or slug test, it is possible to estimate such variables as storativity and transmissivity from well data. This solution is found in such programs as AQTESOLV but is dependent on observational data and does not address the boundary between the confined and unconfined components of the aquifer. The solution is also reliant upon the assumption that the aquifer is fairly thick so transmissivity can be assumed to be constant. Therefore, the solution may be unsuitable for use in those areas where the underlying aquifer is relatively thin (Chen et al, 2006). The Moench and Prickett (1972) solution has been used in analytical models by the United States Geological Survey and used with a variety of equations to create a Modular Finite-Element Model (MODFE) by Cooley (1992), but very little of the flow dynamics in the subsurface is known. In the above research, the analytical models are limited and are not adequate for all applications in the field, but are more suited for larger aquifers undergoing the unconfined-confined condition.

Springer and Bair (1992) examined analytical, semi-analytical, and numerical

models using CAPZONE®, DREAM®, and MODFLOW® respectively, and compared each model's results using a standard data set to predict well capture zones and simulate flow. A stratified-drift aquifer was located and modeled in Wooster, Ohio. The aquifer is considered confined, but is unconfined in sections from lack of an upper confining bed near alluvial fan deposits. The production from the aquifer increased dramatically from 1984 to 1988 from 3.5 to 4.4 million gallons/day, respectively. The models were examined for an accurate calculation of hydraulic head which was compared against the actual value to create a mean absolute error (MAE). Springer and Bair (1992) concluded that the analytical model CAPZONE® was correct in identifying areas that had greater hydraulic head; however the slope of the gradient was too gentle. The semi-analytical model DREAM® produced a similar result showing areas with increased hydraulic head; but the result was even less accurate than CAPZONE®. MODFLOW® produced far more accurate results, as it allows for an in-depth description of the geology of the region including changes in aquifer thickness and hydraulic conductivity which the other models lacked. When compared to the data set MODFLOW® predicted a larger capture zone than either CAPZONE® or DREAM®. Springer and Bair (1992) reasoned that the analytical and semi-analytical models cannot be as accurate as the numerical model because MODFLOW® adjusts for heterogeneity.

1.3 Theoretical Background for a Numerical Model

One equation that has been used to describe an unconfined-confined boundary on a local scale is Girinskii's Potential (Bear, 1972). Girinskii's Potential was developed as

a method to determine the exact location of the unconfined-confined boundary in a mixed aquifer assuming the aquifer is horizontal and under steady-state flow conditions (Bear, 1972). Bear (1972) suggests that Girinskii's Potential has the ability to adequately describe the flow within a horizontal unconfined-confined aquifer.

The equation was later altered and used by Chen et al. (2006) to describe the unconfined-confined boundary in an aquifer that was proximal to a constant head boundary. It is from this altered equation from which the research proposed begins.

In situations where the aquifer changes from one state to another, which usually occurs as the result of excessive pumping of a confined aquifer, very few models have been developed for use on a local scale. Therefore, new and existing equations must be tested and modeled in order to adequately describe these systems.

CHAPTER II

THEORETICAL DEVELOPMENT I: NO-FLOW BOUNDARY

2.1 Calculation of Flow

Calculated by Henry Darcy in 1856, Darcy's Law is one of the most important hydrogeological concepts and is the starting point from which most calculations begin. Darcy's objective was to experimentally calculate the flow rate of water as it traveled through a sandy substrate. The resultant equation is most commonly shown in Eq (1):

$$Q = q \times A = -K(h_1 - h_2)/L \tag{1}$$

where Q represents total flow [L^3/T], q the volumetric flow rate per unit surface area [L/T], A the cross-sectional area, K the hydraulic conductivity of the aquifer [L/T], h_1 and h_2 the hydraulic head [L], and L the distance between h_1 and h_2 [L] (Domenico and Schwartz, 1998).

Darcy's law shows the linear relationship between q and the hydraulic gradient $(h_1 - h_2)/L$, as long as the flow is laminar and the substrate granular and permeable (Domenico and Schwartz, 1998).

2.2 Review of Girinskii's Potential

Girinskii's Potential (Bear, 1972, Chen et al., 2006) has been applied to generally confined aquifers affected by natural or anthropological stresses under steady-state flow conditions. As demands upon these aquifers increase there is a possibility that the hydraulic head may decrease and as a result the water table drops below the upper confining bed. This occurrence would create air pockets within the aquifer which then becomes depressurized and therefore unconfined. Girinskii's Potential allows for a solution to be found for the location of this unconfined-confined boundary, as long as natural and anthropological influences are known numerically. As applied here Girinskii's Potential is found for a multi-layered generally horizontal aquifer in steady-state with a fully penetrating pumping well. Girinskii's Potential for a confined aquifer is expressed in Eq. (2) as:

$$\varphi = Kb(H - b/2) + c, \tag{2}$$

where φ represents Girinskii's Potential, H the hydraulic head [L], b the aquifer thickness [L], and c is a constant depending on the reference used.

A similar equation for an unconfined aquifer is expressed in Eq. (3) as:

$$\varphi = Kh^2/2 + c, \tag{3}$$

where h represents the thickness of the saturated portion of the aquifer [L]. An aquifer that has no recharge and is depleted by pumping would gradually have a decrease of hydraulic head around the pumping well. As this occurs, the hydraulic head becomes equivalent to the elevation of the upper confining bed and the aquifer loses pressurization. Girinskii's Potential predicts that a transition occurs during this process. The potential for that location is shown in Eq. (4) as:

$$\varphi_c = Kb^2/2 + c, \tag{4}$$

and may be located near any area where the hydraulic head has a similar value as the thickness of the aquifer. At any location where φ becomes less than φ_c, $h < b$ and the transition occurs from confined to unconfined (Chen et al., 2006).

Assuming an aquifer is steady-state, confined and extends laterally to a distance where the effects of pumping are not constrained by the aquifer's lateral dimensions the equation, as shown in Eq. (5) is:

$$d\varphi/dr = Kb(dH/dr), \tag{5}$$

where r designates radial distance [L].

2.3 Deriving Flow from Girinskii's Potential

Assuming that water approaches a well from all directions and that the well is fully penetrating then flow can be calculated as shown in Eq. (6).

$$Q = q \times A = 2\pi r K b (dH / dr) = 2\pi r (d\varphi / dr) \tag{6}$$

Q can be related to Girinskii's Potential using the integration of the above equation which is shown in Eq. (7) and yields:

$$\varphi = (Q / 2\pi) \ln r + c\,, \tag{7}$$

where c is a constant.

Presuming that an unconfined area is present in the aquifer around the pumping well an assumption can be made that at some radial distance away from the well $H = b$. This allows Girinskii's Potential to be used for both the unconfined and confined portions of an aquifer to be compared. Taking the difference of these potentials allows for the location of the area where $H = b$ to be found. Assuming at a known radius distance $r = r_0$ the Girinskii's Potential is φ_0. At the unconfined-confined conversion $r = r_c$ and $\varphi = \varphi_c$. Taking the difference of the φ_c and φ_0 and substituting as shown in Eq. (8) yields:

$$\varphi_c - \varphi_0 = (Q / 2\pi) \ln(r_c / r_0) . \quad (8)$$

Solving for r_c from above equation results in Eq. (9):

$$r_c = r_o e^{2\pi(\varphi_c - \varphi_0)/Q} . \quad (9)$$

This equation predicts the radial distance of the boundary between the unconfined and confined parts of the aquifer caused by a pumping well.

2.4 Deriving the Solution of a Well near a No-Flow Boundary

A no-flow boundary located near a pumping well is quantitatively similar to an image pumping well located on the other side of the boundary, with each well being equidistant from that boundary. Such boundaries are non-permeable and assumed to be fully penetrating. Vertical igneous intrusions or structural bodies such as faults are typical causes of such behavior.

An aquifer near a no-flow boundary may be represented by modifying Girinskii's Potential to account for an image pumping well with an identical pumping rate as both situations yield identical results. A separation of flow must occur between the pumping and image wells. The relationship between the pumping well and image well is shown in Eq. (10).

$$\varphi = (Q/2\pi)\ln(rr') + c' \quad (10)$$

r and r' represent the distance the pumping well and image pumping wells are from a monitoring well [L], respectively, and c' is a constant depending on the reference used. A reference point much be designated to determine c'.

At some point all effects of pumping are negated by distance. At a distance of *Re* away from the pumping well there is no drawdown created by pumping. *Re* is then named the radius of the influence of the pumping well (Bear, 1972). For a pumping well that is located at the shortest possible distance L from a no-flow boundary, a reference point A is created that lies on the line connecting the real and image pumping wells. Point A is located a distance *Re* from the real pumping well on the side of the pumping well furthest away from the no-flow boundary. Because there is no drawdown at point A $H = h_0$, where h_0 is the initial piezometeric head in the confined aquifer before pumping begins. The Girinskii's Potential at this point A is $\varphi = Kb(h_0 - b/2)$. Distance can be shown as $r = \mathrm{Re}$ and $r' = \mathrm{Re} + 2L$. Substituting for r and r' into Eq. (10) yields Eq. (11) and Eq. (12):

$$\varphi = Kb(h_0 - b/2) = (Q/2\pi)\ln\left(\mathrm{Re}\times(\mathrm{Re}+2L)\right) + c' \quad (11)$$

or

$$c' = Kb(h_0 - b/2) - (Q/2\pi)\ln\left(\mathrm{Re}\times(\mathrm{Re}+2L)\right) \tag{12}$$

Substituting Eq. (12) into Eq. (10) results in Eq. (13):

$$\varphi = Kb(h_0 - b/2) + (Q/2\pi)\ln\left[\frac{rr'}{\mathrm{Re}\times(\mathrm{Re}+2L)}\right] \tag{13}$$

Whereas the most favorable situation while calculating the unconfined-confined boundary is to know the exact distance of *Re* through field tests and monitoring wells, this is unlikely. Previous attempts have been made to estimate values of *Re* with regard to aquifer dimensions and flow characteristics through semi-empirical and empirical methods. According to Bear (1979) the quantitative estimations for *Re* are:

Semi-Empirical Formulas (see Bear, 1979)

$$\mathrm{Re} = H\sqrt{K/2N}$$

$$\mathrm{Re} = 2.45\sqrt{HKt/n_e}$$

$$\mathrm{Re} = 1.9\sqrt{HKt/n_e}$$

Empirical Formulas (see Bear, 1979)

$$\mathrm{Re} = 3000 s_w \sqrt{K}$$

$$\mathrm{Re} = 575 s_w \sqrt{HK}$$

where N is the amount of water recharging the aquifer through percolation of rainwater into the ground, t is time, n_e is the effective porosity, and s_w is the measurement of the total drawdown.

Replacing φ with its solution above results in Eq. (14).

$$Kb^2/2 = Kb(h_0 - b/2) + (Q/2\pi)\ln\left[\frac{rr'}{\mathrm{Re}\times(\mathrm{Re}+2L)}\right] \qquad (14)$$

All variables except r and r' are found by well tests. Solving the solution for these variables results in Eq. (15).

$$rr' = (\mathrm{Re}^2 + 2\,\mathrm{Re}\,L)\times e^{Kb(-2\pi/Q)(h_0-b)} = u \qquad (15)$$

There are several dimensionless parameters that are necessary to test the accuracy and sensitivity of this equation:

1) $\alpha = Kb^2/Q$

2) $\beta = h_0/b$

3) $\chi = L/\mathrm{Re}$

When the above solution is solved numerically, the boundary between the confined and unconfined areas of the aquifer will appear circular with one location near the monitoring well. An assumption can be made that less water is arriving at the

pumping well as a result of the no-flow boundary. This shortage of water violates the assumptions made earlier in which water approaches the well equally from all directions. The mathematical result is an alteration in the shape of the boundary from a circular shape to that better defined by an oval. A change in the formula must then be made to alter the shape of the boundary. Because the distance from the center of an oval to its parameter is not constant radial flow does not apply. Using the equation for determining an oval's shape r and r' change into $r = (x + L)^2 + y^2$ and $r' = (x - L)^2 + y^2$, which improves the accuracy of the solution as well as allowing traditional *xy* coordinates to be used. Solving the equation for all values of *y* allows for graphical visualization of the boundary. Substituting for r and r' changes the equation to Eq. (16).

$$u = [(x + L)^2 + y^2] \times [(x - L)^2 + y^2] \tag{16}$$

Applying the quadratic equation and simplifying gives the final solution which may be graphed to show the unconfined-confined boundary shown in Eq. (17) to be.

$$\xi = \pm[-(x^2 + L^2) + \sqrt{4x^2L^2 + u^2}], \tag{17}$$

where $y = \pm\sqrt{\xi}$.

CHAPTER III

THEORETICAL DEVELOPMENT II: REGIONAL FLOW

3.1 Deriving Regional Flow from Girinskii's Potential

Building upon the work presented by Chen et al. (2006) an equation showing the effects of regional flow using Girinskii's Potential can be created.

Using the general equation shown above, regional flow is introduced as Eq. (18).

$$\varphi = (Q \ln r) / 2\pi + q'x \tag{18}$$

where q' is altered from its normal dimensions to [L^2/T]. A point a distance of *Re* away the aquifer is unaffected by pumping. Assuming that the coordinates at that point are $x = 0$ and $y = \mathrm{Re}$, taking the derivative of this equation can be shown as Eq. (19).

$$\varphi = (Q \ln \mathrm{Re}) / 2\pi + c' \tag{19}$$

Because this is a boundary between unconfined and confined flow, $\varphi = Kb(h_0 - b/2)$. This allows for a calculation of c' to be acquired. Introducing c' into our first equation compares the value of that equation against the boundary where $\varphi = 0$. As shown in Eq. (20) The equation becomes:

$$\varphi = Kb(h_0 - b/2) + Q\ln(r/\mathrm{Re})/2\pi + q'x\,, \tag{20}$$

where $r = \sqrt{x^2 + y^2}$ is the result of regional flow preventing water from approaching the well uniformly. By further substituting for known values for φ and φ_0, the equation can be shown as Eq. (21).

$$Kb^2/2 = Kb(h_0 - b/2) + Q\ln(\sqrt{x^2 + y^2}/\mathrm{Re})/2\pi + q'x \tag{21}$$

If solved for *y*, the equation becomes Eq. (22).

$$\delta = \ln(\sqrt{x^2 + y^2}/\mathrm{Re}) = 2\pi[Kb^2/2 - Kb(h_0 - b/2)]/Q - q'x \tag{22}$$

Eq. (22) can be further simplified to Eq. (23).

$$e^{\delta} = \sqrt{x^2 + y^2}/\mathrm{Re}\,. \tag{23}$$

The graphical equation can then be found to be Eq. (24).

$$y = \sqrt{(\mathrm{Re}\,e^{\delta})^2 - x^2}\,. \tag{24}$$

Another key dimensionless parameter is necessary here to test for accuracy and sensitivity and is the result of incorporating regional flow, and is shown in Eq. (25).

$$\kappa = q' \mathrm{Re} / Q \tag{25}$$

CHAPTER IV

ANALYTIC SOLUTIONS FOR LOCATING THE UNCONFINED-CONFINED TRANSITION

4.1 Hypothetical Model 1: No-Flow Boundary

Using MATLAB® a model was created to graphically analyze hypothetical unconfined-confined boundaries. After the user establishes values for each variable within the equation the model solves for *y* using a range of *x* values separated at a user-defined interval. The model then uses these *x* and *y* values to graph a multitude of data plots that show the location of the unconfined-confined boundary within a normally confined aquifer. To adequately show the entire unconfined-confined boundary the range of *x* values solved by the equation must be larger than the extent of the boundary. The model was instructed to produce graphs showing the unconfined-confined boundary created from a pumping well and an image pumping well separated by a distance of $2L$, the midpoint of which is the no-flow boundary. Control variables were assumed to be:

b = 20 meters
H_0 = 22 meters
K = 20 meters/day
Q = 500 g/min (Converted to m^3/day automatically by the model)
L = 50 meters
Re = 500 meters.

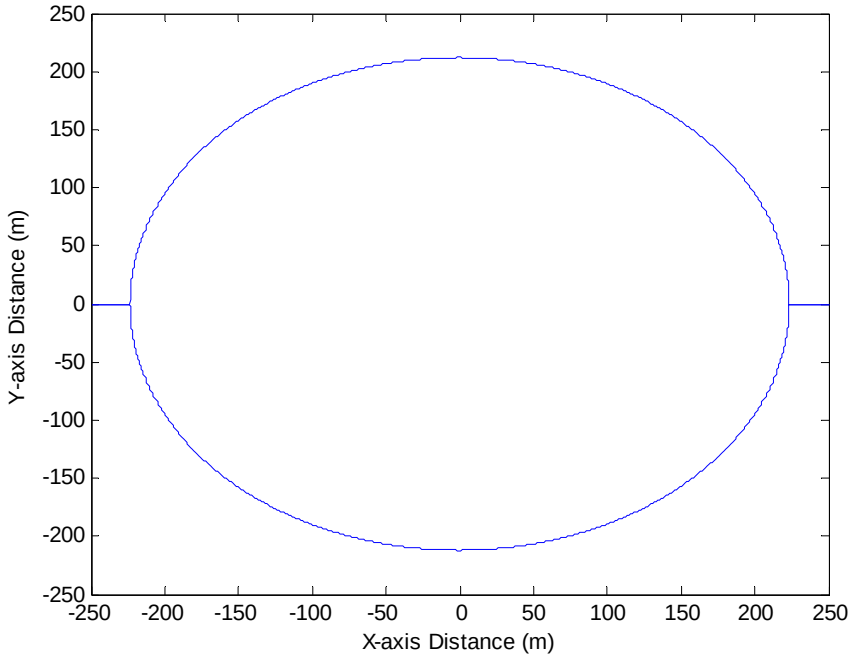

Figure 1. Planar view of the unconfined-confined boundary for an aquifer affected by no-flow boundary.

The control values were substituted into Eq. (17) and are shown in Figure 1. The no-flow boundary is located along the *y*-axis, while the pumping well and image well are located at (-50, 0) and (50, 0), respectively. The unconfined-confined boundary appears circular with an approximate radius of 225 meters. The negative *y*-axis represents the area under study while the positive *y*-axis the image well. The positive *y*-axis does not represent true flow on the other side of the no-flow boundary and is dismissed.

4.1.1 Calculation from $\alpha = Kb^2 / Q$

Values for α were derived by lowering the quantity of water being pumped from the well where the hydraulic conductivity and aquifer thickness remained constant. Simulations were performed which are shown in Figure 2.

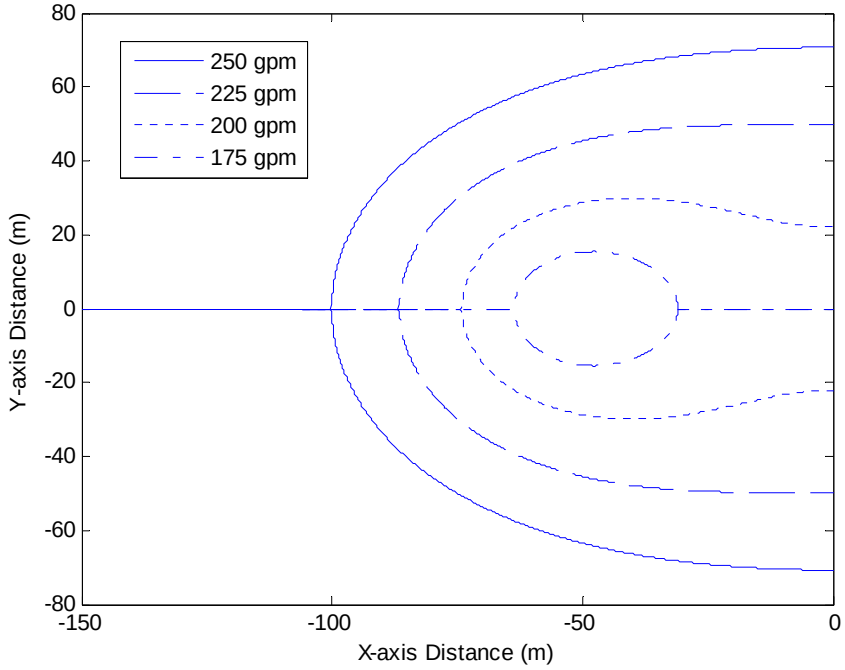

Figure 2. Alpha sensitivity analysis for an aquifer near a no-flow boundary. Control variables were $K = 20$ meters/day and $b = 20$ meters. Pumping rates at (0, 0) were set at values of 250, 225, 200, and 175 gallons/minute and were converted to meters^3/day by the model.

Pumping rates that are above 250 gallons/minute allow the effects of having a pumping well near a no flow boundary to be viewed. At such high rates, both the pumping and image wells act to combine at a single center located at a position

equidistant to both located at the no flow boundary. The reduction of Q from large quantities to 225 gallons/minute results in a reduction of the radius of the unconfined-confined boundary with little change in boundary symmetry. At these rates, the principle effect on the unconfined-confined boundary is the exhaustion of water supplies in close proximity to the no-flow boundary. As the quantity of water withdrawn is reduced to 200 gallons/minute, the boundary begins to lose its circular appearance and the effects of the no-flow boundary become reduced. The unconfined-confined boundary drawdown contacts the no-flow boundary and is increased by the lack of recharge that alters the symmetry of the boundary to a tear-drop shape. As pumping rates are decreased to 175 gallons/minute the unconfined-confined boundary begins to be influenced by the individual well rather than the no-flow boundary. Once pumping rates reach this level the no-flow boundaries' effect is minimal on drawdown and the pumping well can be treated as if the no-flow boundary is not present.

4.1.2 Calculation from $\beta = h_0 / b$

To calculate β, values of h_0 were increased to allow constant aquifer width. The original model and all variables were used as a control and can be viewed in Figure 3.

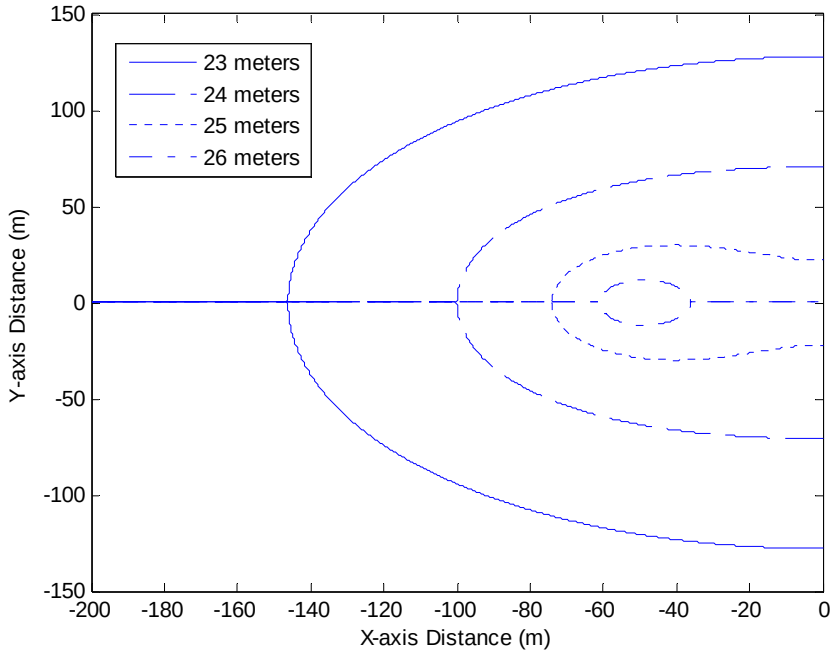

Figure 3. Beta sensitivity analysis for an aquifer near a no-flow boundary. Control variable was $b = 20$ meters. Values substituted for h_0 were 23, 24, 25 and 26 meters.

As the original h_0 is increased from 23 meters the unconfined-confined boundary remains circular until h_0 = 24. As the h_0 is increased further to 25 meters the boundary's shape changes into the teardrop form with the most dominant characteristic being a portion which has been affected by the limited recharge associated with the no-flow boundary. Between 25 and 26 meters, the boundary separates from the no-flow boundary and by 26 meters is found only within a 5 meter radius of the well. At this hydraulic head, the unconfined-confined boundary becomes largely independent of any affect that the no-flow boundary imposes upon drawdown.

4.1.3 Calculation from $\chi = L / \mathrm{Re}$

Mentioned previously, the value of *Re* represents a monitoring well's distance from the pumping well at which no drawdown occurs. A small *Re* indicates that the effect of pumping is not widespread. If L was increased, the well would be farther from the no-flow boundary, and the effects would be lessened. For calculation by the model *Re* was decreased and can be viewed in Figure 4.

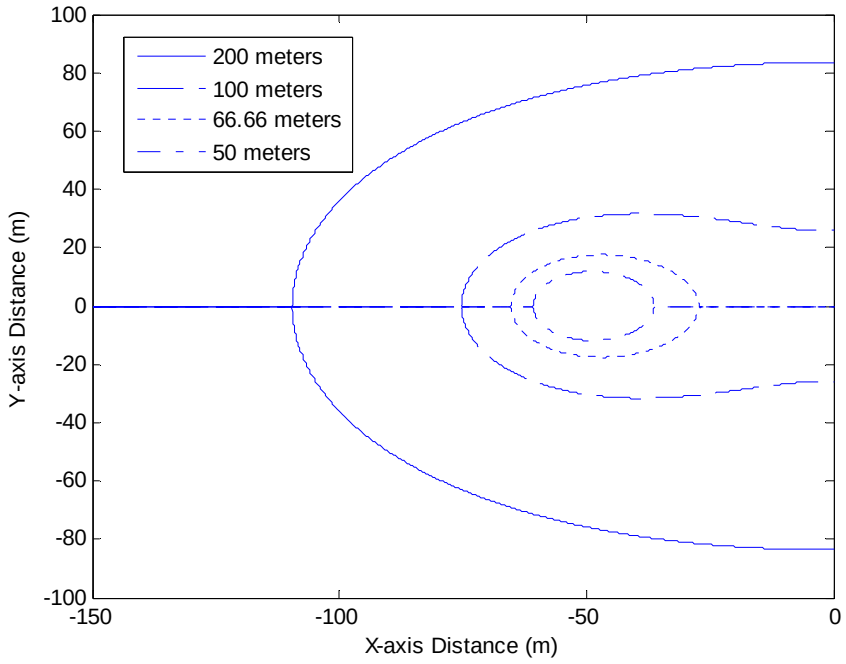

Figure 4. Chi sensitivity analysis for an aquifer near a no-flow boundary. Control variable was $L = 50$. Substituted values for *Re* were 200, 100, 66.66, and 50 meters.

Values for χ were calculated starting with the control model. As seen in Figure 1 (pg. 22), a *Re* of 500 meters creates a circular boundary. For this solution values of *Re* were reduced from 200 meters to show the rapid change between 200 meters to 50

meters. As the values of *Re* are reduced, the circular shape remains until *Re* = 200 meters. At 200 meters the shape of the boundary becomes oval and is slightly elongated along the x-axis. As *Re* is reduced to 100 meters the unconfined-confined boundary begins to become the tear-drop shape seen previously. A reduction of *Re* to 66.66 meters shows the unconfined-confined boundary detach from the no-flow boundary and becomes isolated to the pumping well yet is elongated in the direction of the no-flow boundary. At a *Re* of 50 meters, the no-flow boundary seems to minimally impact the drawdown.

4.2 Creating the Hypothetical Model 2: Regional Flow

Using MATLAB®, a similar solution was presented for a confined aquifer under the influence of regional flow. The model was instructed to produce graphs showing the unconfined-confined boundary using Eq. (22), the control variables and a $q' = 0.006$ meters^2/day flowing parallel to the *x* axis, towards the negative direction. Figure 5 shows a confined aquifer under such conditions with a well located at (0, 0).

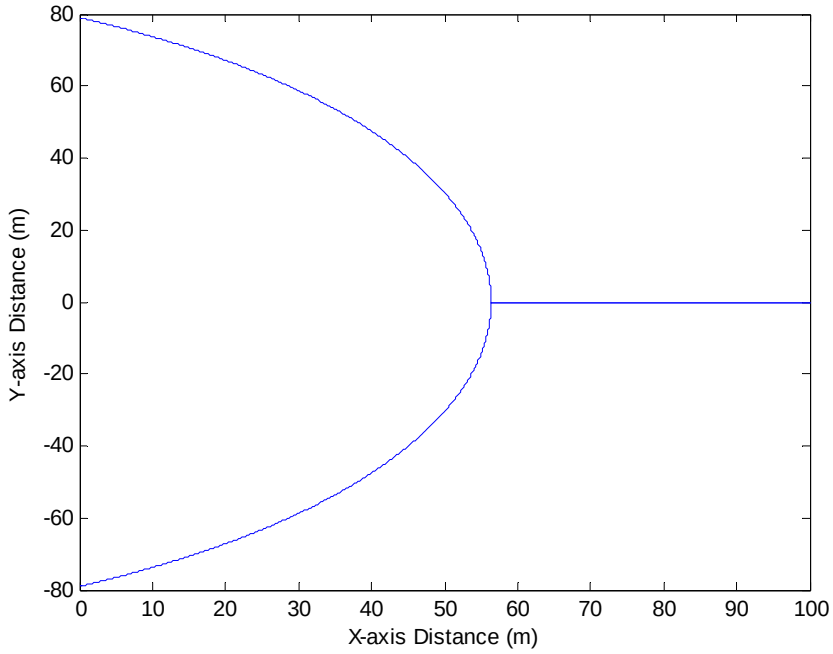

Figure 5. Planar view of the unconfined-confined boundary for an aquifer affected by regional flow.

4.2.1 Calculation from $\alpha = Kb^2 / Q$

Values for α were derived from diminishing the water pumped from the well while K and b values remained constant to show the affect of various pumping rates on the unconfined-confined boundary. The results can be viewed in Figure 6.

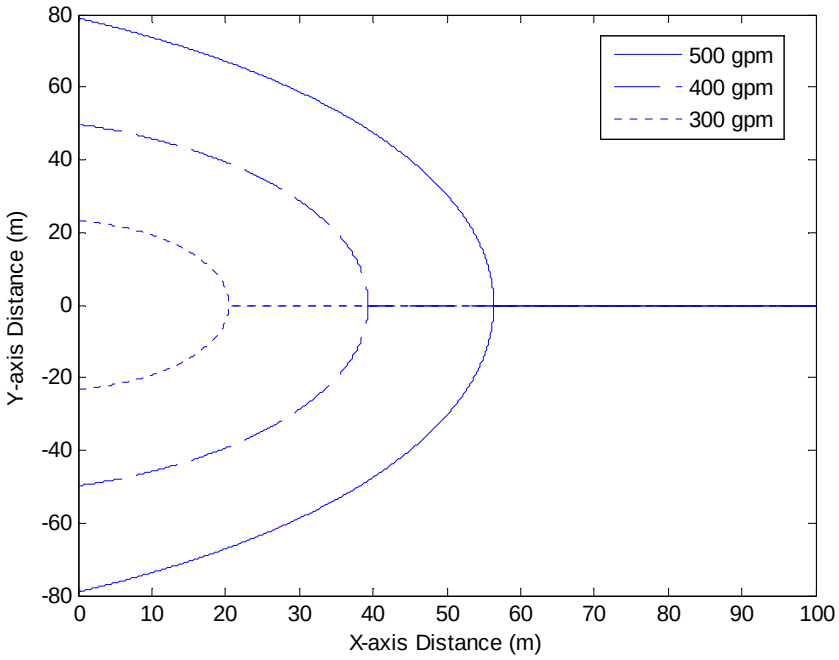

Figure 6. Alpha sensitivity analysis for an aquifer with regional flow. Control variables were $K = 20$ meters/day and $b = 20$ meters. Pumping rates of 500, 400, and 300 gallons/minute were analyzed.

As pumping rates decline, the unconfined-confined boundary reduces in size at approximately the same rate. At 500 gallons per minute, the maximum drawdown on the *x*-axis is approximately 57 meters. As this rate is reduced to 400 and 300 gallons/minute, the drawdown on the *x*-axis is located at 38 and 20 meters respectively and seems to show a change of 18 to 19 meters per 100 gallons/minute.

4.2.2 Calculation from $\beta = h_0 / b$

β values were calculated by maintaining the aquifer thickness at $b = 20$ meters while increasing h_0 values from 23 meters to 26 meters in increments of 1 meter. The results are shown in Figure 7.

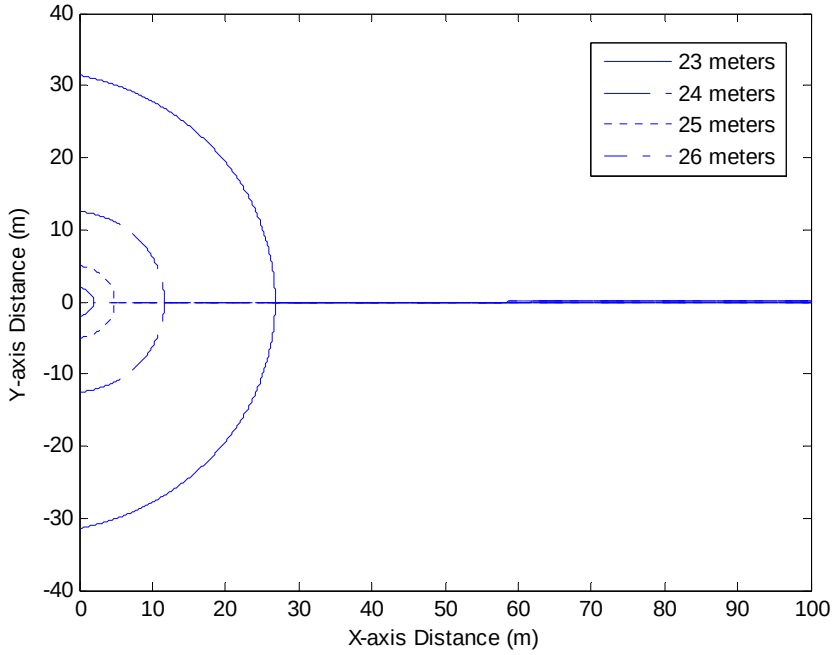

Figure 7. Beta sensitivity analysis for an aquifer with regional flow. Control variable was $b = 20$ meters. h_0 values were 23, 24, 25, and 26 meters.

As h_0 values decrease the size of the unconfined-confined boundary reduces. The largest drawdown shown occurs at a head of 23 meters. As the head increases to 24 meters the unconfined-confined boundary rapidly shrinks, with further increases producing a similar although lesser effect. The closer the upper confining bed is to the

piezometric head level produces an increasingly larger impact on drawdown.

4.2.3 Calculation from $\chi = L / \mathrm{Re}$.

To produce χ values L remained at the control value of 50 meters while the *Re* values were reduced from 400 to 100 meters in 100 meter intervals. The plan view of the change has been shown in Figure 8.

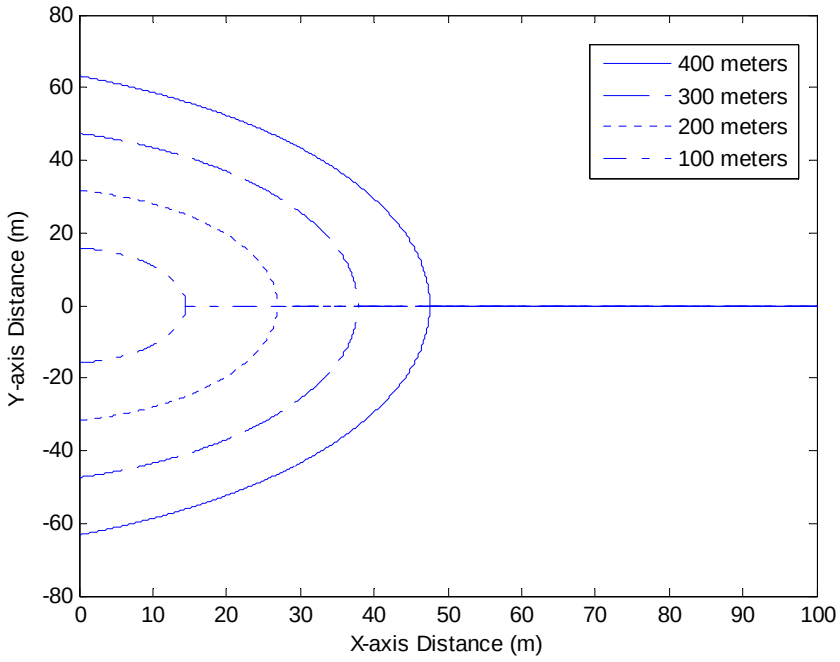

Figure 8. Chi sensitivity analysis for an aquifer with regional flow. Control variable was $L = 50$ meters. *Re* values of 400, 300, 200, and 100 meters were used.

As *Re* values are lowered from 400 to 100 meters the unconfined-confined boundary shrinks. Because *Re* is the location closest to the well that is unaffected by drawdown, a decrease in *Re* would represent that location being more proximal to the pumping well. The decreases in *Re* reduce the size of the boundary at a rate that seems proportional.

4.2.4 Calculation from $\kappa = q' \mathrm{Re}/Q$

The change of q' represents the change in regional flow affecting the aquifer and hence recharge. The calculation of κ allows for the comparison of the major factors affecting the aquifer. Values for *Re* and Q remained constant while q' values were assumed to be the maximum and minimum values that occur most often, 0.01 and 0.002 meters^2/day respectively. The model also calculated the median value of 0.006 meters^2/day. The results predicted by the model are shown in Figure 9.

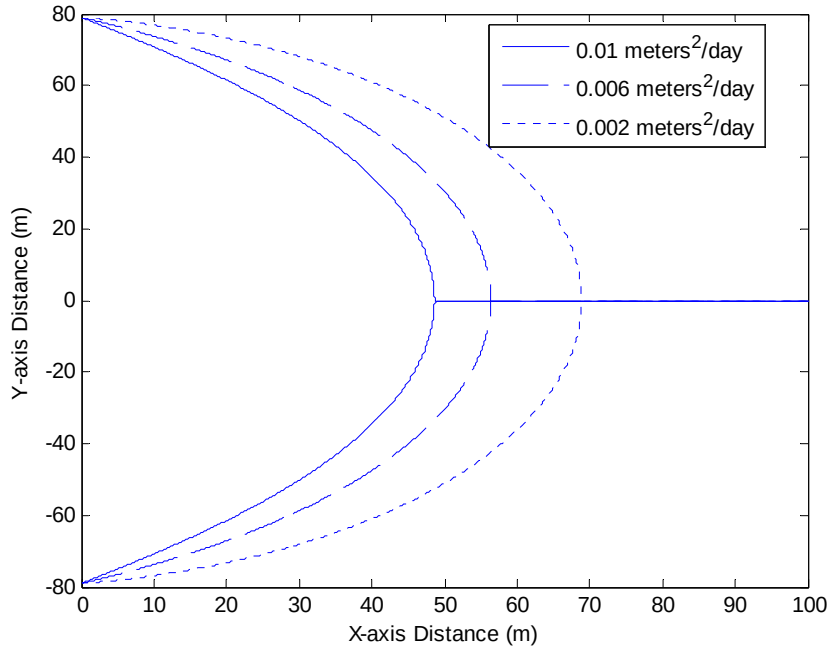

Figure 9. Kappa sensitivity analysis for an aquifer with regional flow. Control variables were *Re* = 500 meters and $Q = 500$ gallons/minute. q' values were 0.01, 0.006 and 0.002 meters^2/day.

At the minimum amount of normal regional flow of 0.002 meters^2/day, an unconfined-confined boundary is located nearly 70 meters away from the pumping well along the *x*-axis. As regional flow is increased to the median range of 0.006 meters^2/day, a rapid reduction of the size of the boundary occurs. At the maximum regional flow of 0.01 meters^2/day the size of the boundary has been reduced to almost 50 meters along the *x*-axis but is reduced at a lesser rate. The effect of an increase in regional flow upon the aquifer causes the unconfined-confined boundary to reduce in size but as regional flow increases, the change in size by the boundary becomes less.

CHAPTER V

DISCUSSION AND CONCLUSIONS

As the human population increases the demand for water supplies will cause an increase in pumping rates from groundwater reservoirs. As a consequence, many previously confined aquifers may become dewatered or unconfined after long-term heavy pumping. Such an unconfined-confined conversion problem has not been fully investigated before and is the focus of this thesis. The objective of this thesis is to use both analytical and numerical modeling to investigate groundwater flow in an unconfined-confined aquifer system under various circumstances including the no-flow lateral boundary effect and the regional flow influence. Ideally, this effort will lead to the ultimate objective of predicting how much water can be sustainably pumped from an aquifer with no harm.

This study has used Girinskii's Potential in combination with MATLAB® to carry out the steady-state calculation of groundwater flow in unconfined-confined aquifers under natural or anthropogenic stresses. The model depicts how changes in aquifer dimensions, hydraulic properties, regional flow rates, and pumping rates affect the size and shape of the confined-unconfined boundary within a hypothetical aquifer. The model provides a sustainable pumping rate which is the maximum rate that will not cause the conversion from a confined aquifer condition to an unconfined aquifer condition. Based on this study, the following conclusions can be made:

1. Larger pumping rates increase the size of the unconfined-confined boundary,

as expected.

2. The unconfined-confined conversion is quite sensitive to the distance between the piezometric surface and the upper confining bed when that distance is small, and the sensitivity lessens as that distance increases.
3. As hydraulic conductivity and regional flow rates increase, the size of the unconfined-confined boundary reduces.
4. Pumping rate is the dominating factor for controlling the size of the unconfined-confined boundary in comparison to the regional flow.
5. The presence of a no-flow boundary alters the normally elliptical shape of the unconfined-confined boundary.

The usage of Girinskii's Potential has been limited to mostly hypothetical situations, yet it could apply to many aquifers that exhibit water level declines; some declines so severe that unsaturated portions form within the aquifer. How the unsaturated flow will affect the saturated flow has not been considered in present research of unconfined-confined flow and should be explored in the future. Furthermore, when drawdowns are significantly large, a three-dimensional approach will improve the accuracy of the present two-dimensional approach. Such three-dimensional flow problems probably have to be solved using a numerical model such as MODFLOW®. Further research into the unconfined-confined conversion problem should incorporate other factors such as vertical recharge and heterogeneity in the aquifer. Hopefully, a groundwater model that includes most necessary hydrological processes and is sufficiently accurate can be established to predict the long-term behavior of an

unconfined-confined aquifer system. In particular, such a model is expected to provide a maximum pumping rate that is sustainable for withdrawing groundwater from a confined aquifer without causing the dewatering of such an aquifer.

REFERENCES

Bear, J. 1972. *Dynamics of Fluids in Porous Media*. New York: Elsevier.

Bear, J. 1979. *Hydraulics of Groundwater*. New York: McGraw-Hill.

Birtles, A.B., and M.J. Reeves. 1977. Computer modeling of regional groundwater systems in the confined-unconfined flow regime. *Journal of Hydrology* 34, no. 1-2: 97-127.

Chen, C.X., L.T. Hu, and X.S. Wang. 2006. Analysis of steady ground water flow toward wells in a confined-unconfined aquifer. *Ground Water* 44, no. 4: 609-612.

Cooley, R.L. 1992. A modular finite-element model (MODFE) for areal and axisymmetric ground-water flow problems, Part 2: Derivation of finite-element equations and comparisons with analytical solutions. Techniques of Water-Resources Investigations of the United States Geological Survey. Book 6, A4, 81-108.

Domenico, P.A., and F.W. Schwartz. 1998. *Physical and Chemical Hydrogeology*. New York: Wiley, 34.

Elango, K., and K. Swaminathan. 1980. A finite-element model for concurrent confined-unconfined zones in an aquifer. *Journal of Hydrology* 46, no. 3-4: 289-299.

Kashef, A.I., 1971. Overpumped artesian wells among a well group. *Water Resources Bulletin* 7, no. 5: 981-990.

Moench, A.F., and T.A. Prickett. 1972. Radial flow in an infinite aquifer undergoing conversion from artesian to water table conditions. *Water Resources Research* 8, no. 2: 494-499.

Naymik, T.G. 1979. The application of a digital model for evaluating the bedrock water resources of the Maumee River Basin, northwestern Ohio. *Ground Water* 17, no. 5: 429–445.

Rushton, K.R., and A. Turner. 1975. Numerical analysis of pumping from confined-unconfined aquifers. *Water Resources Bulletin* 10, no. 6: 1255-1269.

Rushton, K.R. 1974. Extensive pumping from unconfined aquifers. *Water Resources Bulletin* 10, no. 1: 32-41.

Springer, A.E., and E.S. Bair. 1992. Comparison of methods used to delineate capture zones of wells: 2. stratified-drift buried-valley aquifer. *Ground Water* 30, no. 6: 908-917.

Visocky, A.P. 1982. Impact of Lake Michigan allocations on the Cambrian-Ordovician aquifer system. *Ground Water* 20, no. 6: 668-674.

Walton, W.C. 1964. Future water-level declines in deep sandstone wells in Chicago region. *Ground Water* 2, no. 1: 13-20.

APPENDIX A

MATLAB PROGRAM FOR UNCONFINED-CONFINED BOUNDARY NEAR A NO-FLOW ZONE

```
disp('Prepare to enter variables for a no-flow boundary system ')

    %Input aquifer, pumping and system variables for no-flow boundary and aquifer
    b = input('Enter the thickness of the aquifer (b) in meters  ');
    Ho = input('Enter the elevation difference between the water table and lower
confining bed (Ho) in meters  ');
    K = input('Enter the hydraulic conductivity (K) in meters/day  ');
    Q1 = input('Enter the pumping rate (Q) in gallons/minute  ');
    L = input('Enter the distance pumping well (L) is from no-flow boundary in meters
');
    Re = input('Enter the distance at which no observable drawdown occurs (Re) in
meters  ');

    %Input x-axis domain, used to determine figure scale
    x1 = input('Enter the maximum x-value for the negative axis (use negative sign)  ');
    x2 = input('Enter the maximum x-value for the positive axis  ');
    XInterval = input('Enter the x-interval (data calculated every x meters, usually 1 or
less)  ');
    x = [x1:XInterval:x2];

    %Flow Equations for no-flow and relevant conversions
    Q = Q1.*5.450992992; %Used to convert Q from gallons/minute into cubic
meters/day, as required by the equations
    e = 2.718281828459;
    Alpha = Re*(Re+2*L)*e.^((-2*pi/Q)*K*b*(Ho-b));
    y = (-(x.^2+L.^2) + ((4*x.^2*L.^2)+ Alpha.^2).^(1/2)).^(1/2);
    y1 = -y
    plot(x,y)
    hold on
    plot(x,y1)
    hold off
    xlabel('X-axis Distance (m)')
    ylabel('Y-axis Distance (m)')
    title('\bf Aerial View of an Unconfined-Confined Boundary', 'FontSize', 14)
end
```

APPENDIX B

MATLAB PROGRAM FOR UNCONFINED-CONFINED BOUNDARY WITH REGIONAL FLOW

```
disp('Prepare to enter variables for a regional flow system  ')

      %Input aquifer, pumping and system variables for regional flow
      b = input('Enter the thickness of the aquifer (b) in meters  ');
      Ho = input('Enter the elevation difference between the water table and lower
confining bed (Ho) in meters  ');
      K = input('Enter the hydraulic conductivity (K) in meters/day  ');
      Q1 = input('Enter the pumping rate (Q) in gallons/minute  ');
      qo = input('Enter the regional (or volumetric) flow (q) in meters/day  ');
      Re = input('Enter the distance at which no observable drawdown occurs (Re) in
meters  ');

     %Input x-axis domain, used to determine figure scale
      x1 = input('Enter the maximum x-value for the negative axis (use negative sign)  ');
      x2 = input('Enter the maximum x-value for the positive axis  ');
      XInterval = input('Enter the x-interval (data calculated every x meters, usually 1 or
less)  ');
      x = [x1:XInterval:x2];

      %Flow Equations for regional flow and relevant conversions
      Q = Q1.*5.450992992; %Used to convert Q from gallons/minute into cubic
meters/day, as required by the equations
      e = 2.718281828459;
      Alpha = ((2*pi)/Q)*(((1/2)*K*b.^2)-(K*b*(Ho-b/2)))-qo*x;
      y = (((Re*e.^Alpha).^2)-x.^2).^(1/2)
      y1 = -y
      plot(x,y)
      hold on
      plot(x,y1)
      hold off
      xlabel('X-axis Distance (m)')
      ylabel('Y-axis Distance (m)')
      title('\bf Aerial View of an Unconfined-Confined Boundary', 'FontSize', 14)
```

VITA

Name:	Kent Langerlan
Address:	Department of Geology and Geophysics, Texas A&M University College Station, Texas 77843-3115
Email Address:	klangerlan@hotmail.com
Education:	B.A. Geology, State University of New York at Geneseo, 2003
	M.S. Geology, Texas A&M University, 2009